Phenomenology of GPDs: status and perspectives

Jakub Wagner

Theoretical Physics Department
National Centre for Nuclear Research, Warsaw

Corigliano Calabro, Italy, 26 September 2022

Deep Inelastic Scattering $e\,p \to e\,X$

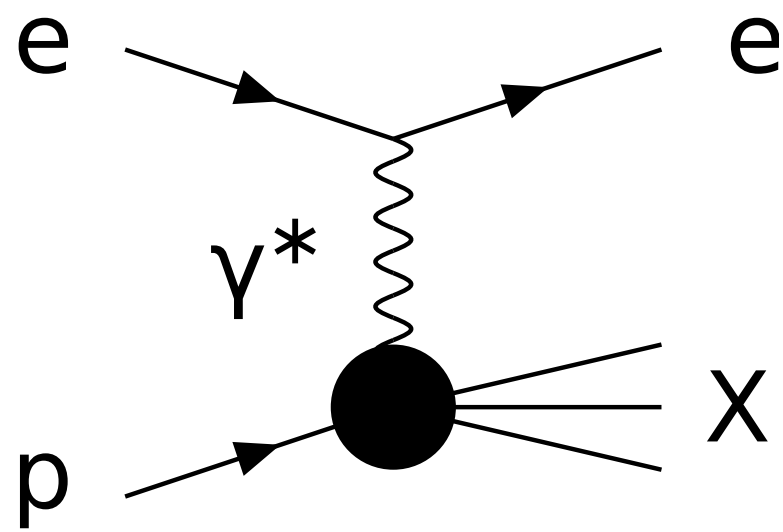

In the Björken limit i.e. when the photon virtality $Q^2 = -q^2$ and the squared hadronic c.m. energy $(p+q)^2$ become large, with the ratio $x_B = \frac{Q^2}{2p\cdot q}$ fixed, the **cross section factorizes** into a **hard partonic subprocess** calculable in the pertutbation theory, and a **parton distributions (PDFs)**.

DIS

- Parton distributions encode the distribution of **longitudinal** momentum and polarization carried by quarks, antiquarks and gluons within fast moving hadron
- PDFs don't provide infomation about how partons are distributed in the transverse plane and ...
- about how important is the orbital angular momentum in making up the total spin of the nucleon.
- For the last 20+ years - growing interest in the **exclusive** scattering processes, which may shed some light on these issues through the generalized parton distributions (GPD).

DVCS

The simplest and best known process is Deeply Virtual Compton Scattering: $e\,p \to e\,p\,\gamma$

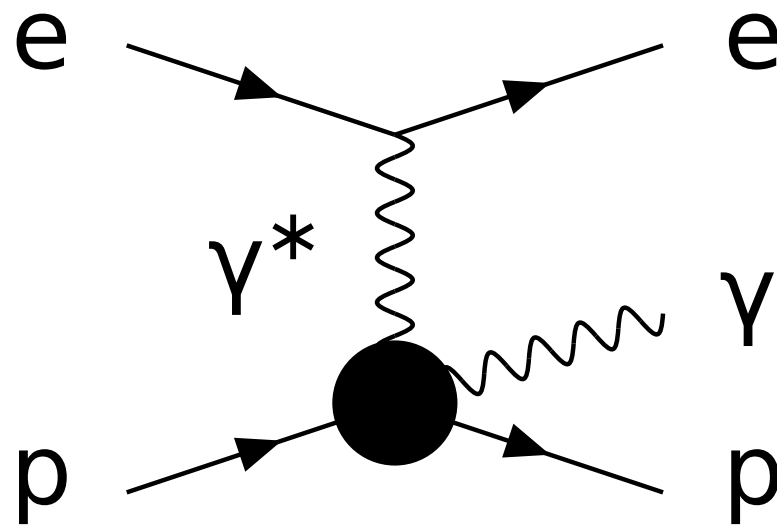

Factorization into **GPDs** and perturbative coefficient function - on the level of **amplitude**.

DIS : $\sigma = \textbf{PDF} \otimes \textbf{partonic cross section}$

DVCS : $\mathcal{M} = \textbf{GPD} \otimes \textbf{partonic amplitude}$

DVCS

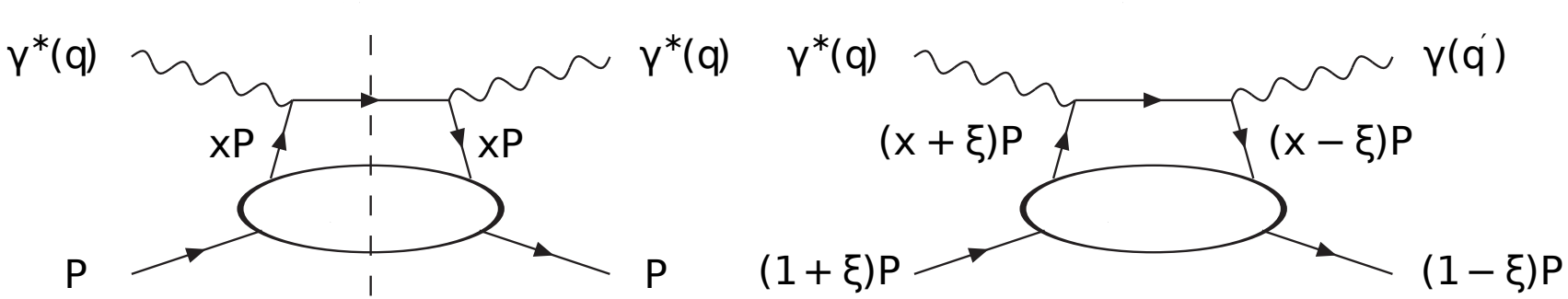

- **Cross section** of Deep Inelastic Scattering is given by the **imaginary** part of the **left** diagram
- **Amplitude** of Deeply Virtual Compton Scattering is given by **right** diagram

Symmetric variables

$$P = \frac{p + p'}{2} \quad , \quad \bar{q} = \frac{q + q'}{2}$$

Generalized Bjorken variable:

$$\xi = \frac{-\bar{q}^2}{2\bar{q} \cdot P} \approx \frac{x_B}{2 - x_B} \quad , \quad x_B = \frac{Q^2}{2q \cdot p}$$

momentum transfer between proton initial and final state:

$$\mathbf{t} = (p' - p)^2$$

In the convenient reference frame, where P has only positive time- and z-components, and light vector are defined as:

$$v_+ = (1, 0, 0, 1)\frac{1}{\sqrt{2}} \quad , \quad v_- = (1, 0, 0, -1)\frac{1}{\sqrt{2}}$$

(-2ξ) has an interpretation of the fraction of momentum transport in "+" direction (ξ - **skewness**).

GPD definition.

$$
\begin{aligned}
F^q &= \frac{1}{2}\int \frac{dz^-}{2\pi}\, e^{ixP^+z^-} \langle p'|\, \bar{q}(-\frac{1}{2}z)\, \gamma^+ q(\frac{1}{2}z)\, |p\rangle \Big|_{z^+=0,\,\mathbf{z}=0} \\
&= \frac{1}{2P^+}\left[H^q(x,\xi,t)\, \bar{u}(p')\gamma^+ u(p) + E^q(x,\xi,t)\, \bar{u}(p')\frac{i\sigma^{+\alpha}\Delta_\alpha}{2m} u(p) \right], \\
F^g &= \frac{1}{P^+}\int \frac{dz^-}{2\pi}\, e^{ixP^+z^-} \langle p'|\, G^{+\mu}(-\frac{1}{2}z)\, G_\mu{}^+(\frac{1}{2}z)\ |p\rangle \Big|_{z^+=0,\,\mathbf{z}=0} \\
&= \frac{1}{2P^+}\left[H^g(x,\xi,t)\, \bar{u}(p')\gamma^+ u(p) + E^g(x,\xi,t)\, \bar{u}(p')\frac{i\sigma^{+\alpha}\Delta_\alpha}{2m} u(p) \right],
\end{aligned}
$$

- interpretation, ERBL, DGLAP

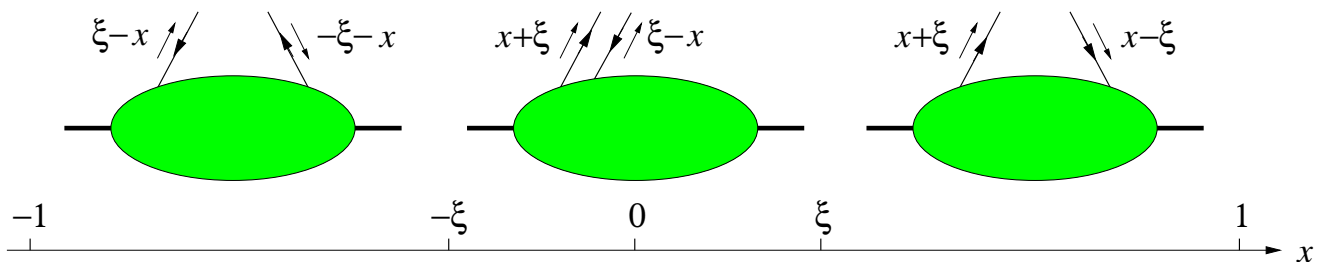

- Factorization scale dependance,
- Three variables x, ξ, t .

GPD - properties,

- Forward limit:

$$\begin{aligned} H^q(x,0,0) &= q(x)\,, \qquad \text{for} \qquad x>0\,, \\ H^q(x,0,0) &= -\bar{q}(x)\,, \qquad \text{for} \qquad x<0\,, \\ H^g(x,0,0) &= xg(x)\,, \end{aligned}$$

  similarly for polarized disributions and PDFs.

- Reduction to form factors:

$$\int_{-1}^{1} dx\, H^q(x,\xi,t) = F_1^q(t), \qquad \int_{-1}^{1} dx\, E^q(x,\xi,t) = F_2^q(t),$$

  where the Dirac and Pauli form factors

$$\langle p'|\,\bar{q}(0)\gamma^\mu q(0)\,|p\rangle = \bar{u}(p')\left[F_1^q(t)\,\gamma^\mu + F_2^q(t)\,\frac{i\sigma^{\mu\alpha}\Delta_\alpha}{2m}\right]u(p),$$

- Ji sum rule:

$$\lim_{t\to 0}\int_{-1}^{1} dx\; x\,[H_f(x,\xi,t) + E_f(x,\xi,t)] = 2J_f$$

  where J_f is fraction of the proton spin carried by quark f (including spin and orbital angular momentum).

Energy momentum tensor and D-term

- Gravitational Form Factors:

$$\langle p', s'|\hat{T}^a_{\mu\nu}(x)|p, s\rangle = \bar{u}'\Big[A^a(t)\,\frac{P_\mu P_\nu}{m} + J^a(t)\,\frac{i\,P_{\{\mu}\sigma_{\nu\}\rho}\Delta^\rho}{2m} + \mathbf{D^a(t)}\,\frac{\Delta_\mu\Delta_\nu - g_{\mu\nu}\Delta^2}{4m} + m\,\bar{c}^a(t)g_{\mu\nu}\Big]u\; e^{i(p'-p)x}.$$

- Form Factor $\mathbf{D(t)}$ connected to pressure
- fixed-t dispersion relation for DVCS

$$Re\mathcal{H}(\xi,t) = \mathbf{\Delta(t)} + \mathrm{P.V.}\int_0^1 \frac{1}{\pi} Im\mathcal{H}(x,t)\left(\frac{1}{\xi - x} \mp \frac{1}{\xi + x}\right)\mathrm{d}x\ .$$

with some approximations: $\mathbf{\Delta(t)} \sim \sum_q \mathbf{D^q(t)} + \ldots$ First attempts made (Burkert et al, Nature 557 (2018)), but difficult to perform in a model independent way.

Impact parameter representation

At $\xi = 0 \qquad \Rightarrow \qquad -t = \Delta_\perp^2$:

$$H(x, \mathbf{b}_\perp) = \int \frac{d^2\mathbf{\Delta}_\perp}{(2\pi)^2} e^{-i\mathbf{b}_\perp \cdot \mathbf{\Delta}_\perp} H(x, 0, -\mathbf{\Delta}_\perp)$$

can be interpreted as probability of finding a parton with longitudinal momentum fraction x at a given $\mathbf{b}_\perp$.

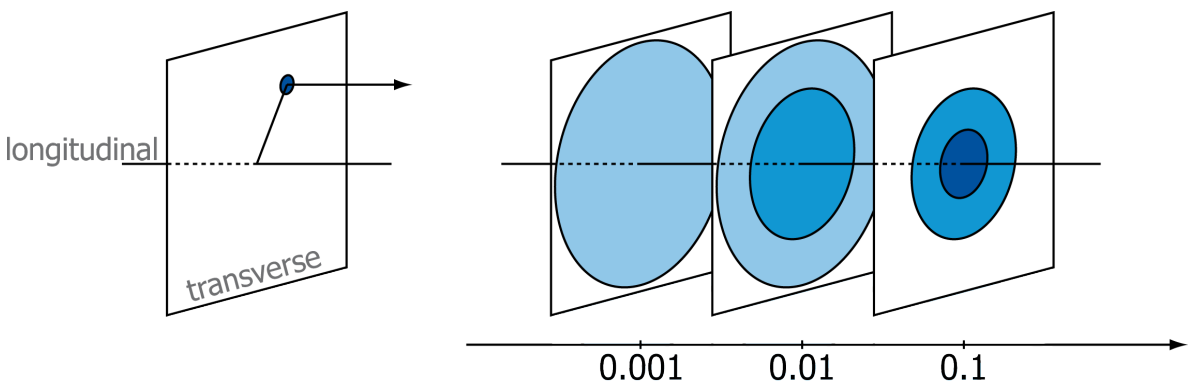

DVCS - Coefficient functions and Compton Form Factors

CFFs are the GPD dependent quantities which enter the amplitudes. They are defined through relations:

$$\mathcal{A}^{\mu\nu}(\xi,t) = -e^2 \frac{1}{(P+P')^+}\,\bar{u}(P')\left[g_T^{\mu\nu}\left(\mathcal{H}(\xi,t)\,\gamma^+ + \mathcal{E}(\xi,t)\,\frac{i\sigma^{+\rho}\Delta_\rho}{2M}\right) + i\epsilon_T^{\mu\nu}\left(\widetilde{\mathcal{H}}(\xi,t)\,\gamma^+\gamma_5 + \widetilde{\mathcal{E}}(\xi,t)\,\frac{\Delta^+\gamma_5}{2M}\right)\right] u(P)\,,$$

,where:

$$\mathcal{H}(\xi,t) \quad = \quad + \int_{-1}^{1} dx \left(\sum_q T^q(x,\xi) H^q(x,\xi,t) + T^g(x,\xi) H^g(x,\xi,t) \right)$$

GPDs enter through convolutions! At LO in α_S:

$$^{DVCS}T^q = -e_q^2 \frac{1}{x+\xi-i\varepsilon} - (x \to -x)$$

$$^{DVCS}Re(\mathcal{H}) \sim P \int \frac{1}{x+\xi} H^q(x,\xi,t)\,, \qquad ^{DVCS}Im(\mathcal{H}) \sim i\pi H^q(\xi,\xi,t)$$

DVCS Observables

- DVCS and Bethe-Heitler

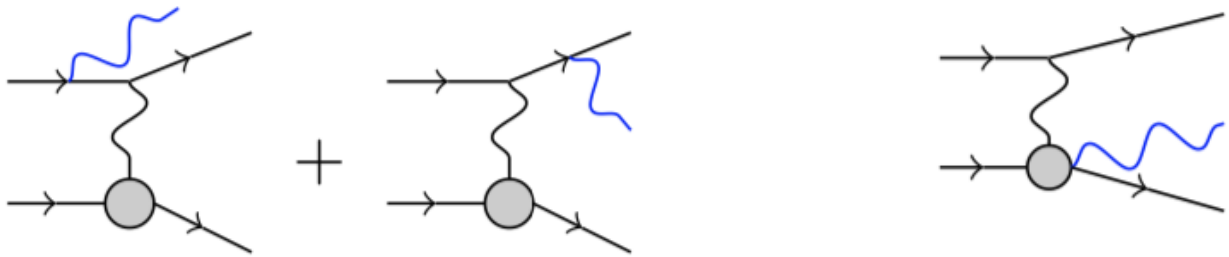

- The $lp \to lp\gamma$ cross section on an unpolarized target for a given beam charge, e_l in units of the positron charge and beam helicity $h_l/2$ can be written as :

$$d\sigma^{h_l,e_l}(\phi) = d\sigma_{\rm UU}(\phi)\left[1 + h_l A_{\rm LU,DVCS}(\phi) + e_l h_l A_{\rm LU,I}(\phi) + e_l A_{\rm C}(\phi)\right] ,$$

One can define various asymmetries:

$$A_{\rm C}(\phi) = \frac{1}{4d\sigma_{\rm UU}(\phi)}\left[(d\sigma^{\overset{+}{\rightarrow}} + d\sigma^{\overset{+}{\leftarrow}}) - (d\sigma^{\overset{-}{\rightarrow}} + d\sigma^{\overset{-}{\leftarrow}})\right] .$$

$$\begin{aligned} A_{\rm LU,I}(\phi) &= \frac{1}{4d\sigma_{\rm UU}(\phi)}\left[(d\sigma^{\overset{+}{\rightarrow}} - d\sigma^{\overset{+}{\leftarrow}}) - (d\sigma^{\overset{-}{\rightarrow}} - d\sigma^{\overset{-}{\leftarrow}})\right] , \\ A_{\rm LU,DVCS}(\phi) &= \frac{1}{4d\sigma_{\rm UU}(\phi)}\left[(d\sigma^{\overset{+}{\rightarrow}} - d\sigma^{\overset{+}{\leftarrow}}) + (d\sigma^{\overset{-}{\rightarrow}} - d\sigma^{\overset{-}{\leftarrow}})\right] . \end{aligned}$$

Observables

$$
\begin{aligned}
A_C^{\cos\phi} &\propto \mathsf{Re}\left[F_1\mathcal{H} + \xi(F_1+F_2)\widetilde{\mathcal{H}} - \frac{t}{4m^2}F_2\mathcal{E}\right], \\
A_{LU,I}^{\sin\phi} &\propto \mathsf{Im}\left[F_1\mathcal{H} + \xi(F_1+F_2)\widetilde{\mathcal{H}} - \frac{t}{4m^2}F_2\mathcal{E}\right], \\
A_{UL,I}^{\sin\phi} &\propto \mathsf{Im}\left[\xi(F_1+F_2)(\mathcal{H}+\frac{\xi}{1+\xi}\mathcal{E}) + F_1\widetilde{\mathcal{H}} - \xi(\frac{\xi}{1+\xi}F_1 + \frac{t}{4M^2}F_2)\widetilde{\mathcal{E}}\right], \\
A_{LL,I}^{\cos\phi} &\propto \mathsf{Re}\left[\xi(F_1+F_2)(\mathcal{H}+\frac{\xi}{1+\xi}\mathcal{E}) + F_1\widetilde{\mathcal{H}} - \xi(\frac{\xi}{1+\xi}F_1 + \frac{t}{4M^2}F_2)\widetilde{\mathcal{E}}\right], \\
A_{LL,DVCS}^{\cos(0\phi)} &\propto \mathsf{Re}\Big[4(1-\xi^2)\big(\mathcal{H}\widetilde{\mathcal{H}}^* + \widetilde{\mathcal{H}}\mathcal{H}^*\big) - 4\xi^2\big(\mathcal{H}\widetilde{\mathcal{E}}^* + \widetilde{\mathcal{E}}\mathcal{H}^* + \widetilde{\mathcal{H}}\mathcal{E}^* + \mathcal{E}\widetilde{\mathcal{H}}^*\big) \\
&\qquad -4\xi\big(\frac{\xi^2}{1+\xi} + \frac{t}{4M^2}\big)\big(\mathcal{E}\widetilde{\mathcal{E}}^* + \widetilde{\mathcal{E}}\mathcal{E}^*\big)\Big], \\
A_{UT,DVCS}^{\sin(\phi-\phi_s)} &\propto \Big[\mathsf{Im}\left(\mathcal{H}\mathcal{E}^*\right) - \xi\mathsf{Im}\left(\widetilde{\mathcal{H}}\widetilde{\mathcal{E}}^*\right)\Big], \\
A_{UT,I}^{\sin(\phi-\phi_s)\cos\phi} &\propto \mathsf{Im}\Big[-\frac{t}{4M^2}\big(F_2\mathcal{H} - F_1\mathcal{E}\big) + \xi^2\big(F_1 + \frac{t}{4M^2}F_2\big)\big(\mathcal{H}+\mathcal{E}\big) \\
&\qquad -\xi^2\big(F_1+F_2\big)\big(\widetilde{\mathcal{H}} + \frac{t}{4M^2}\widetilde{\mathcal{E}}\big)\Big].
\end{aligned}
$$

DVCS data

Table 3: DVCS data used in this analysis.

No.	Collab.	Year	Ref.	Observable		Kinematic dependence	No. of points used / all
1	HERMES	2001	13	A_{LU}^{+}		ϕ	10 / 10
2		2006	119	$A_{C}^{\cos i\phi}$	$i=1$	t	4 / 4
3		2008	120	$A_{C}^{\cos i\phi}$	$i=0,1$	x_{Bj}	18 / 24
				$A_{UT,\mathrm{DVCS}}^{\sin(\phi-\phi_S)\cos i\phi}$	$i=0$		
				$A_{UT,\mathrm{I}}^{\sin(\phi-\phi_S)\cos i\phi}$	$i=0,1$		
				$A_{UT,\mathrm{I}}^{\cos(\phi-\phi_S)\sin i\phi}$	$i=1$		
4		2009	121	$A_{LU,\mathrm{I}}^{\sin i\phi}$	$i=1,2$	x_{Bj}	35 / 42
				$A_{LU,\mathrm{DVCS}}^{\sin i\phi}$	$i=1$		
				$A_{C}^{\cos i\phi}$	$i=0,1,2,3$		
5		2010	122	$A_{UL}^{+,\sin i\phi}$	$i=1,2,3$	x_{Bj}	18 / 24
				$A_{LL}^{+,\cos i\phi}$	$i=0,1,2$		
6		2011	123	$A_{LT,\mathrm{DVCS}}^{\cos(\phi-\phi_S)\cos i\phi}$	$i=0,1$	x_{Bj}	24 / 32
				$A_{LT,\mathrm{DVCS}}^{\sin(\phi-\phi_S)\sin i\phi}$	$i=1$		
				$A_{LT,\mathrm{I}}^{\cos(\phi-\phi_S)\cos i\phi}$	$i=0,1,2$		
				$A_{LT,\mathrm{I}}^{\sin(\phi-\phi_S)\sin i\phi}$	$i=1,2$		
7		2012	124	$A_{LU,\mathrm{I}}^{\sin i\phi}$	$i=1,2$	x_{Bj}	35 / 42
				$A_{LU,\mathrm{DVCS}}^{\sin i\phi}$	$i=1$		
				$A_{C}^{\cos i\phi}$	$i=0,1,2,3$		
8	CLAS	2001	14	$A_{LU}^{-,\sin i\phi}$	$i=1,2$	—	0 / 2
9		2006	125	$A_{UL}^{-,\sin i\phi}$	$i=1,2$	—	2 / 2
10		2008	126	A_{LU}^{-}		ϕ	283 / 737
11		2009	127	A_{LU}^{-}		ϕ	22 / 33
12		2015	128	A_{LU}^{-}, A_{UL}^{-}, A_{LL}^{-}		ϕ	311 / 497
13		2015	129	$d^4\sigma_{UU}^{-}$		ϕ	1333 / 1933
14	Hall A	2015	117	$\Delta d^4\sigma_{LU}^{-}$		ϕ	228 / 228
15		2017	118	$\Delta d^4\sigma_{LU}^{-}$		ϕ	276 / 358
16	COMPASS	2018	56	b		—	1 / 1
						SUM:	2600 / 3970

DVCS data

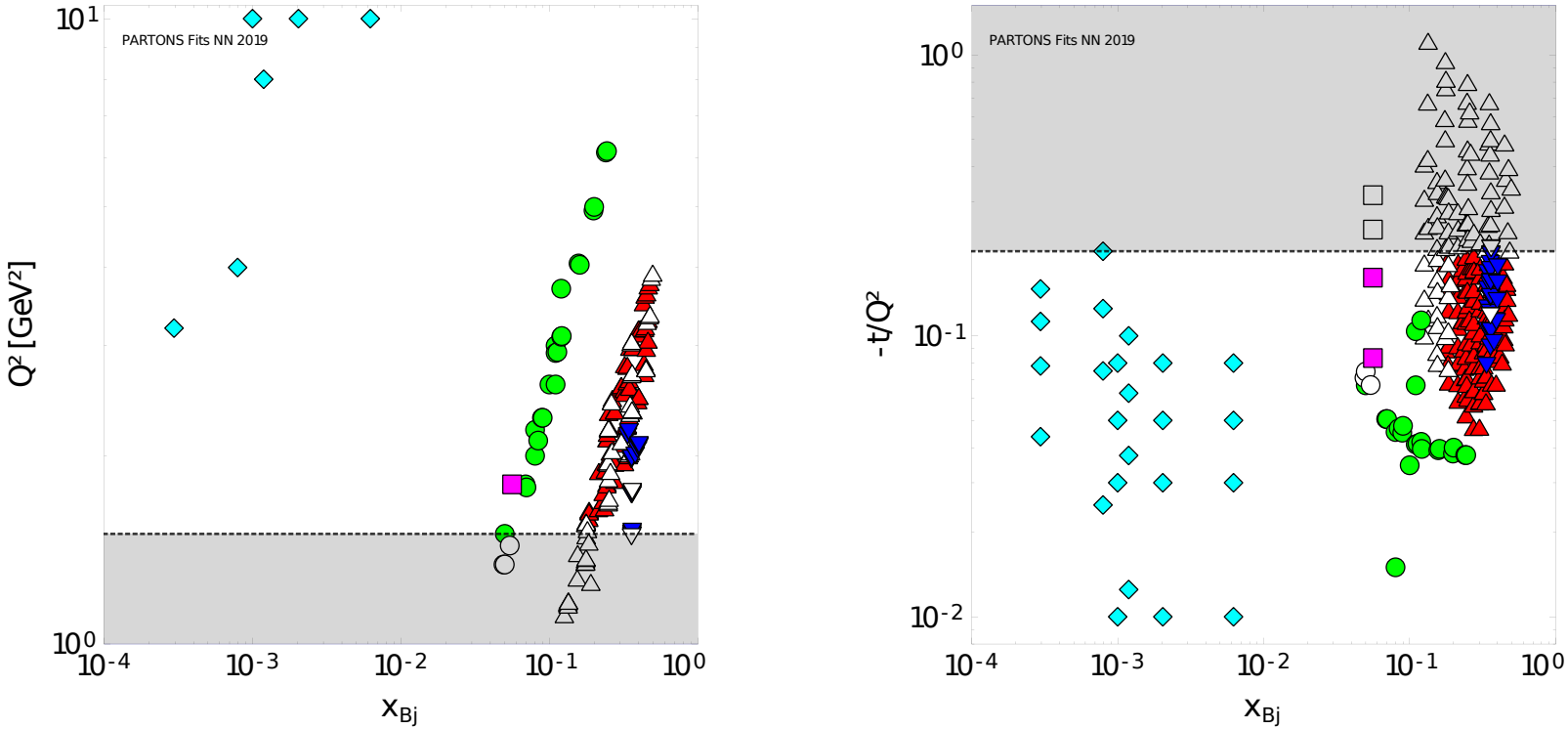

Figure: Coverage of the (x_{Bj}, Q^2) (left) and $(x_{\mathrm{Bj}}, -t/Q^2)$ (right) phase-spaces by the experimental data used in DVCS CFFs fit. The data come from the Hall A (▼, ▽), CLAS (▲, △), HERMES (●, ○), COMPASS (■, □) and HERA H1 and ZEUS (◆, ◇) experiments. The gray bands (open markers) indicate phase-space areas (experimental points) being excluded from this analysis due to the cuts.

Example of parametric fit

H.Moutarde, P.Sznajder and JW, Eur.Phys.J. C78 (2018)

- Border function:
  For the GPDs H^q and $\widetilde{H}^q$ at $\xi = 0$ we use an Ansatz that is commonly used in phenomenological analyses of GPDs:

$$G^q(x,0,t) = \mathrm{pdf}_G^q(x)\ \exp(f_G^q(x)t)\ .$$

  The profile function, $f_G^q(x)$, fixes the interplay between the x and t variables, and it is given by:

$$f_G^q(x) = A_G^q \log(1/x) + B_G^q(1-x)^2 + C_G^q(1-x)x\ ,$$

- Skewness function:

$$g_G^q(x,\xi,t) = \frac{G^q(x,\xi,t)}{G^q(x,0,t)}\ ,$$

  In our case:

$$G^q(x,x,t) = G^q(x,0,t)\ g_G^q(x,x,t)\ ,$$

  We assume the following form (suggested by F. Yuan, Phys. Rev. D69)

$$g_G^q(x,x,t) \equiv g_G^q(x,t) = \frac{a_G^q}{(1-x^2)^2}\left(1 + t(1-x)(b_G^q + c_G^q \log(1+x))\right)\ ,$$

PDFs

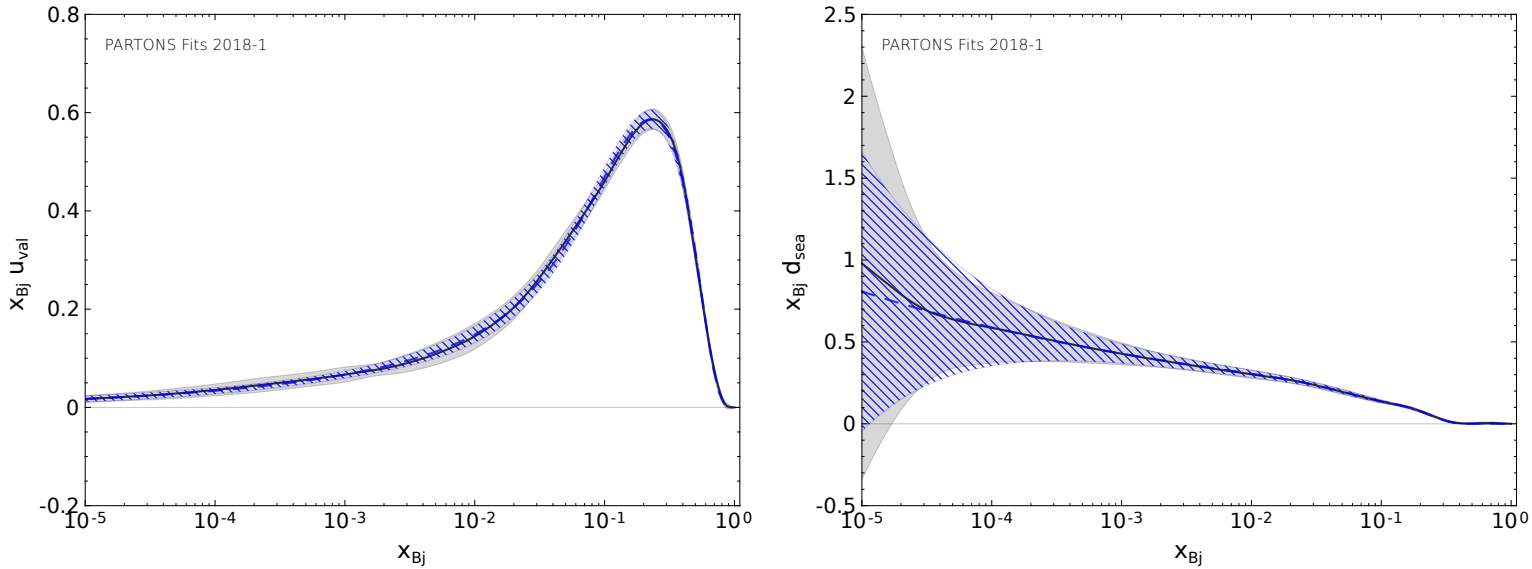

Figure: Comparison between PDF sets by NNPDF group and our parameterizations. The left plot is for u_{val} quarks, while the right one is for d_{sea} quarks. For a given figure, the black solid curve with the grey band representing 68% confidence level is for PDFs by NNPDF group, while the blue dashed curve with the hatched band is for our fit. The curves are evaluated at $Q^2 = 2\ \mathrm{GeV}^2$.

Form Factors - parameters of $f_G^q(x)$ fitted to elastic data.

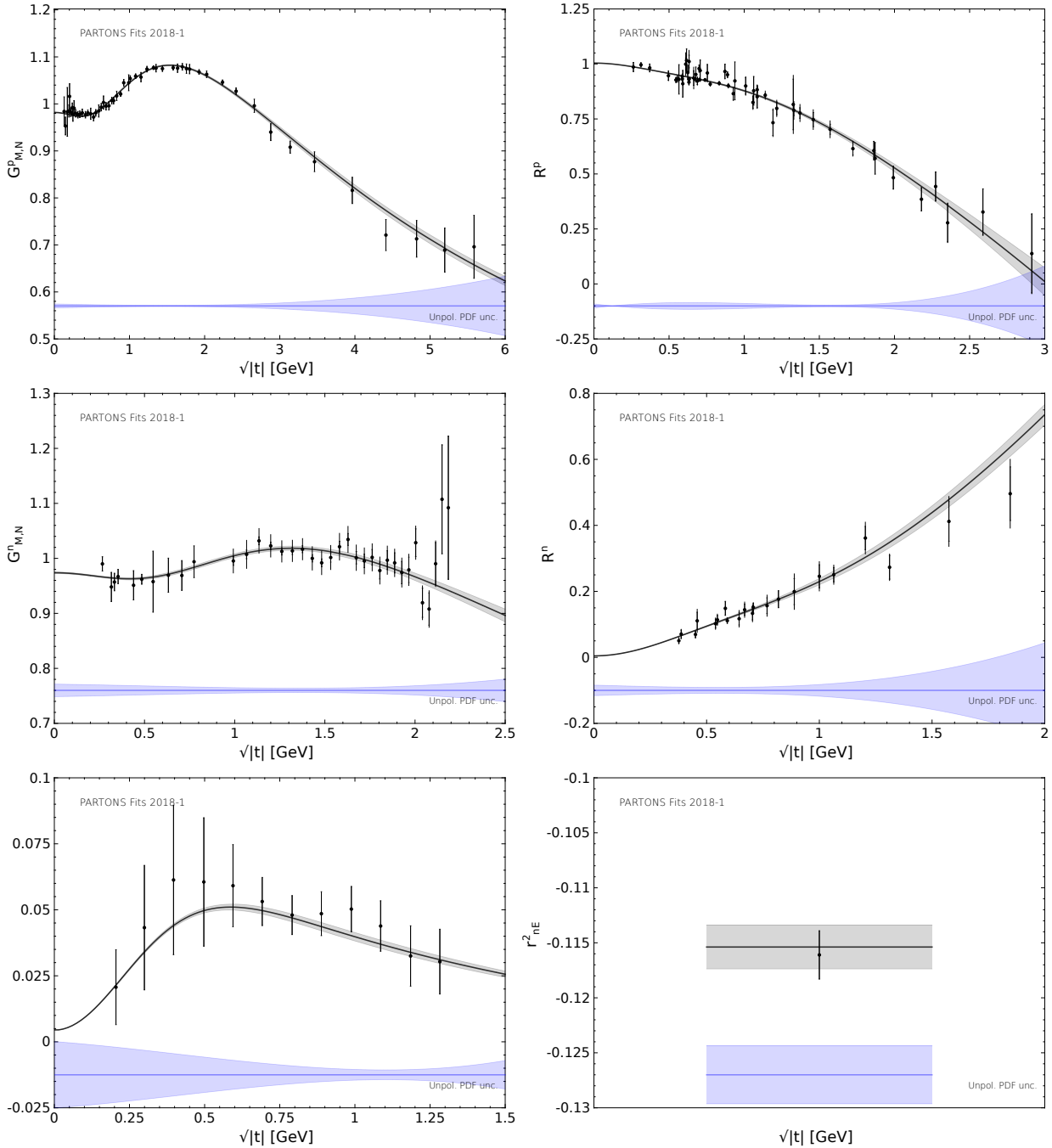

fit results

Table 5: Values of the parameters fitted to DVCS data together with estimated uncertainties coming from those data, (un-)polarized PDFs and EFFs. Two last columns indicate the limits in which the minimization routine was allowed to vary the corresponding parameters. In addition, exemplary values of b_G^q and c_G^q parameters evaluated at $Q^2 = 2$ GeV^2 from Eqs. (62) and (63) are given.

Parameter	Mean	Data unc.	Unpol. PDF unc.	Pol. PDF unc.	EFF unc.	Limit min	Limit max
$a_H^{q_{\rm val}}$	0.81	0.04	0.17	0.02	< 0.01	0.2	2.0
$a_H^{q_{\rm sea}}$	0.99	0.01	0.02	< 0.01	< 0.01	0.2	2.0
$a_{\widetilde{H}}^{q}$	1.03	0.04	0.30	0.24	0.01	0.2	2.0
$N_{\widetilde{E}}$	-0.46	0.10	0.09	0.06	0.01	-10	10
$A_H^{q_{\rm sea}}$	2.56	0.23	0.30	0.09	0.03	0.1	10
$B_H^{q_{\rm sea}}$	-5		at the limit			-5	20
$C_H^{q_{\rm sea}}$	34	27	49	14	3	-5	200
$A_{\widetilde{H}}^{u_{\rm val}}$	0.77	0.12	0.30	0.23	0.07	0.1	10
$B_{\widetilde{H}}^{u_{\rm val}}$	-0.02	0.26	0.75	0.24	0.15	-5	20
$C_{\widetilde{H}}^{u_{\rm val}}$	-0.92	0.07	0.44	0.24	0.04	-5	200
$A_{\widetilde{H}}^{d_{\rm val}}$	0.64	0.24	0.30	0.28	0.05	0.1	10
$B_{\widetilde{H}}^{d_{\rm val}}$	-1.19	0.45	0.91	0.98	0.22	-5	20
$C_{\widetilde{H}}^{d_{\rm val}}$	-0.55	0.24	0.26	0.27	0.10	-5	200
$b_H^{u_{\rm val}}$	-0.36	0.10	0.15	0.04	0.01	—	—
$c_H^{u_{\rm val}}$	11.2	3.1	2.7	1.1	0.3	—	—
$b_H^{d_{\rm sea}}$	-0.222	0.062	0.090	0.022	0.006	—	—
$c_H^{d_{\rm sea}}$	14	4	15	1	1	—	—

For the central PDF and EFF replicas the minimum value of the χ^2 function is 2346.3 for 2600 experimental points and 13 free parameters, which gives the reduced value equal to $2346.3/(2600-13) \approx 0.91$.

fit vs experiments

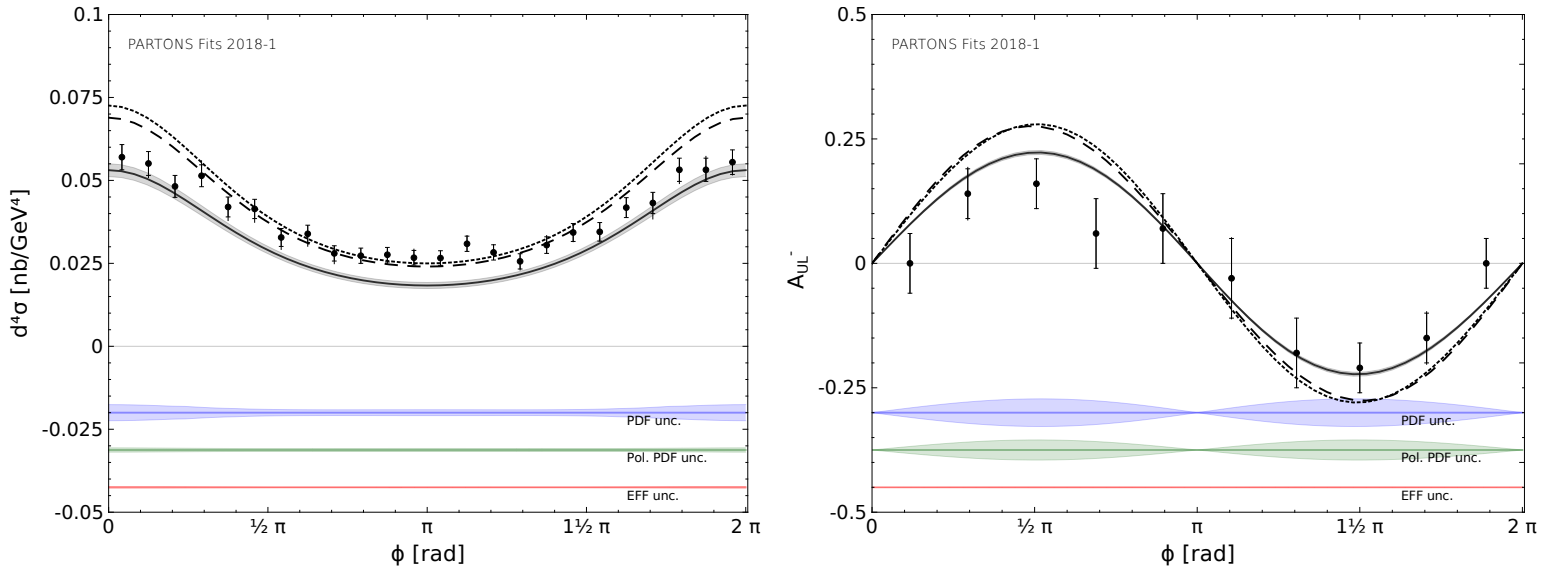

Figure: Comparison between the results of this analysis, some selected GPD models and experimental data published by Hall A (left) and CLAS (right). The solid curves and the gray bands surrounding those curves are for the results of this analysis and 68% confidence levels for the uncertainties coming from DVCS data, respectively. The corresponding bands for (un-)polarized PDFs and EFFs are indicated by the labels. The dotted curve is for the GK GPD model, while the dashed one is for VGG. The curves are evaluated at the kinematics of experimental data.

Compton Form Factors

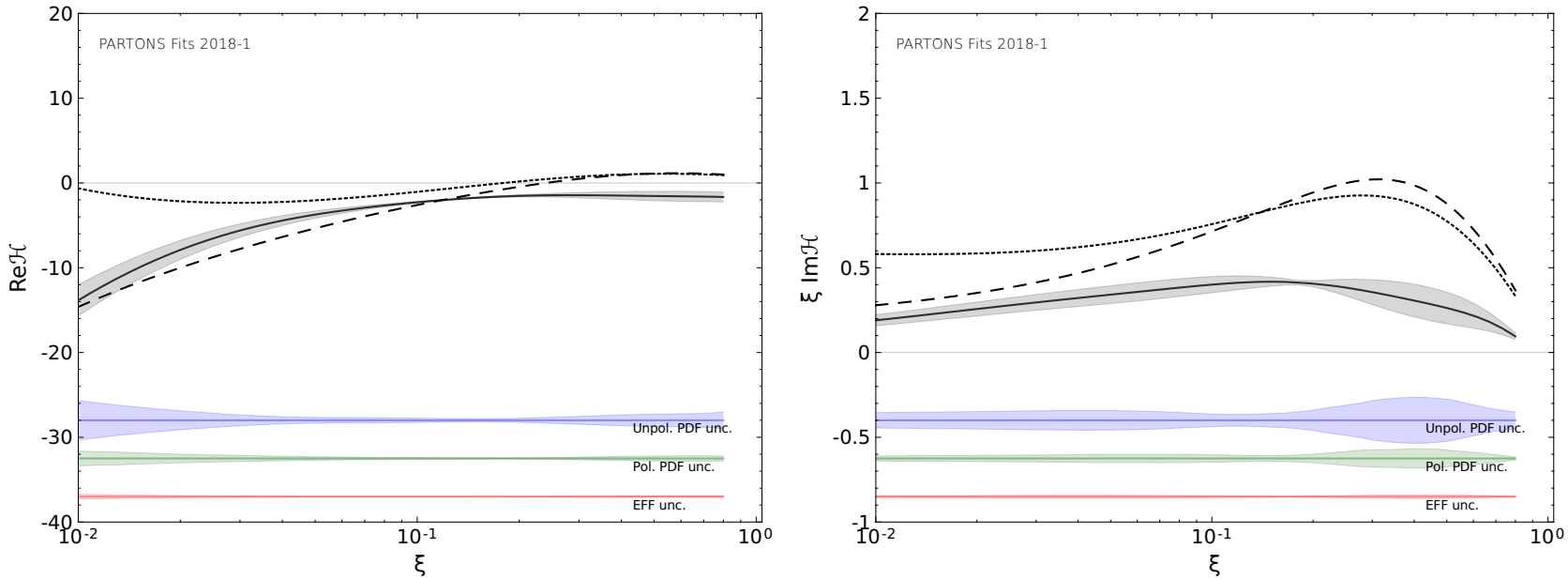

Figure: Real (left) and imaginary (right) parts of the CFF $\mathcal{H}$ obtained in this work as a function of ξ at $t = -0.3\ \mathrm{GeV}^2$ and $Q^2 = 2\ \mathrm{GeV}^2$.

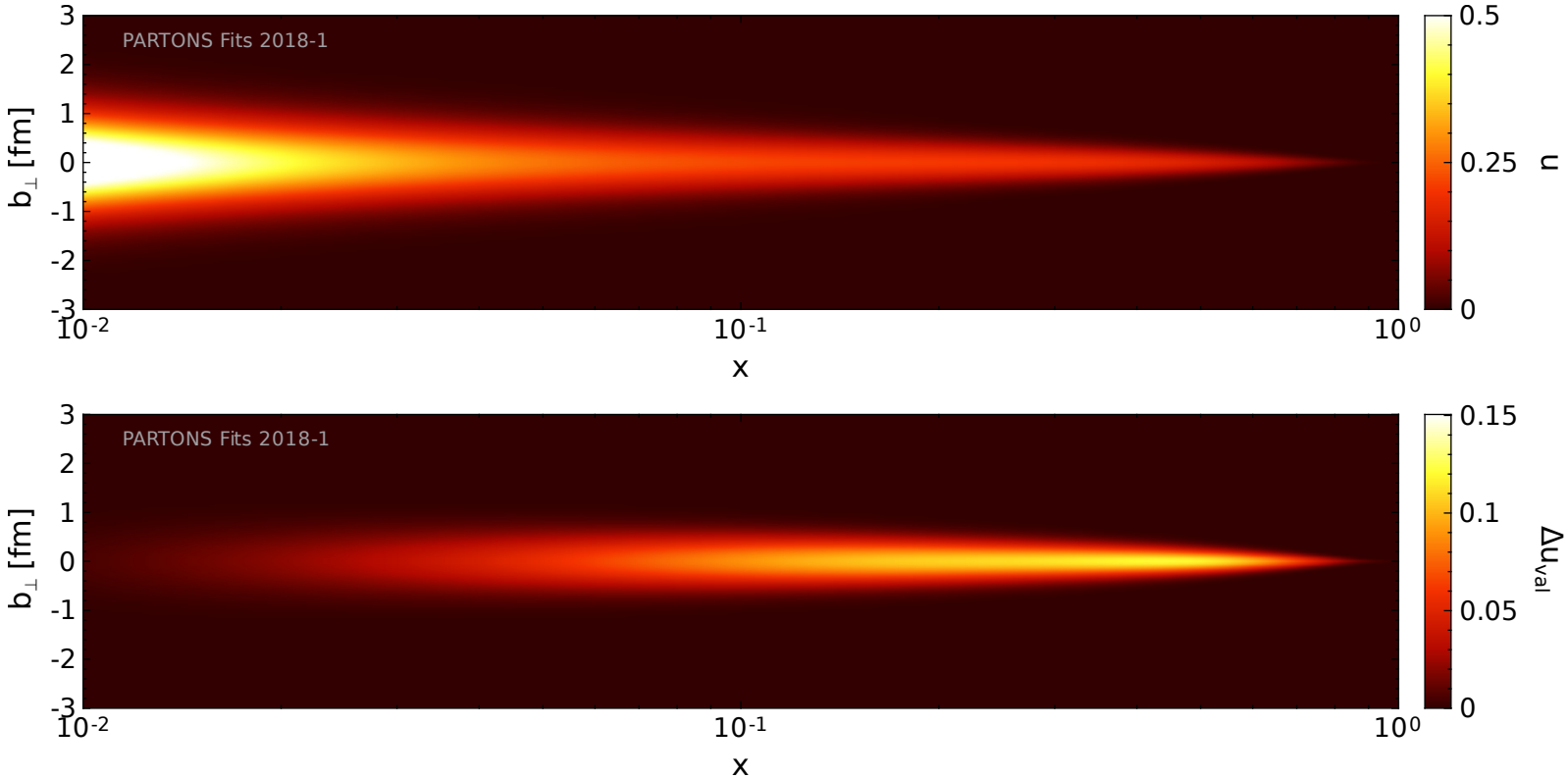

Figure: Position of up quarks in an unpolarized proton (upper plot) and longitudinal polarization of those quarks in a longitudinally polarized proton (lower plot) as a function of the longitudinal momentum fraction x. For the lower plot only the valence contribution is shown.

Fit with ANN + Genetic algorithm

H. Moutarde, P. Sznajder, J. Wagner, Eur.Phys.J. C79 (2019)

- ANNs

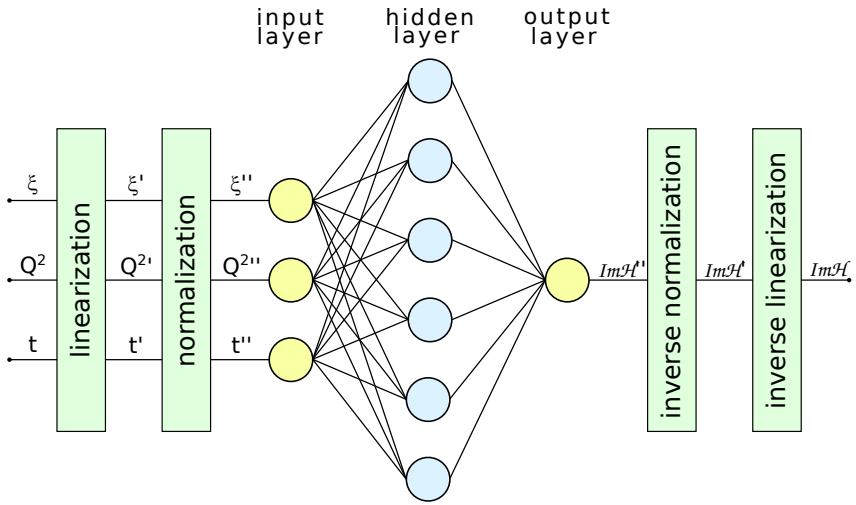

Figure: Scheme of a single neural network that is used in this analysis to represent either the real or the imaginary part of a single CFF.

- Genetic algorithm

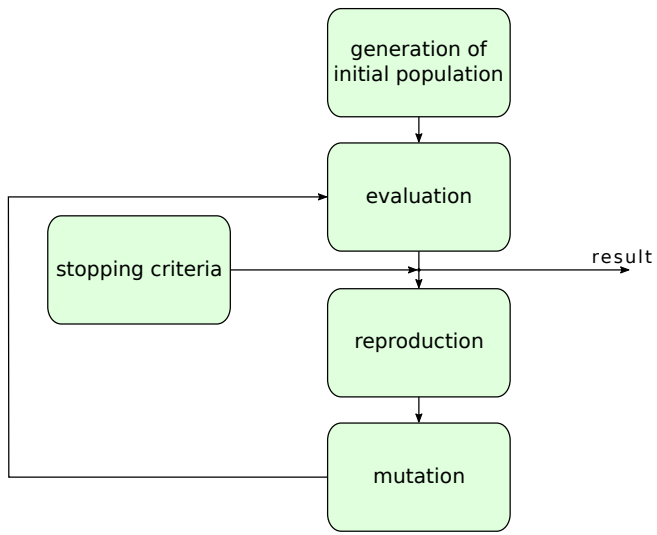

Observables

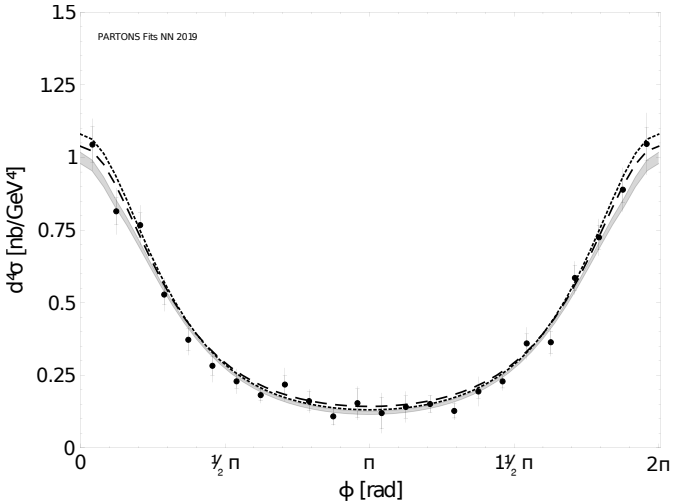

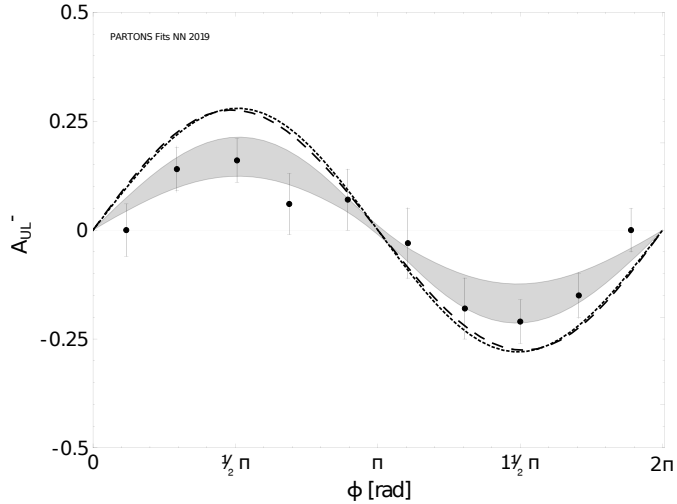

Figure: CLAS data for $d^4\sigma^-_{UU}$ at $x_{\mathrm{Bj}} = 0.244$, $t = -0.15\ \mathrm{GeV}^2$ and $Q^2 = 1.79\ \mathrm{GeV}^2$ (left) and for A^-_{UL} at $x_{\mathrm{Bj}} = 0.2569$, $t = -0.23\ \mathrm{GeV}^2$, $Q^2 = 2.019\ \mathrm{GeV}^2$ (right). The gray bands correspond to the results of this analysis. The dotted curve is for the GK GPD model, while the dashed one is for VGG.

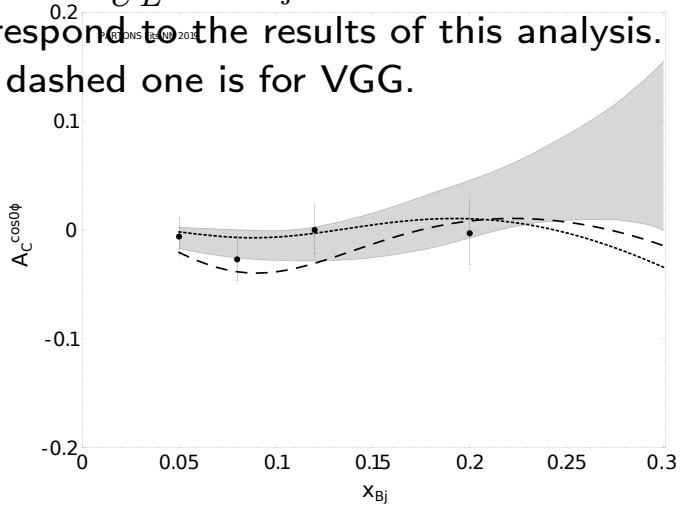

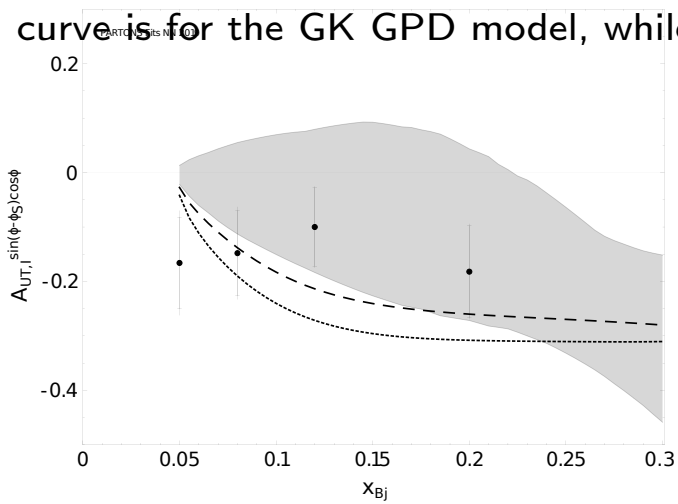

Figure: HERMES data for $A_C^{\cos 0\phi}$ (left) and $A_{UT,\mathrm{I}}^{\sin(\phi-\phi_S)\cos\phi}$ (right) at $t = -0.12\ \mathrm{GeV}^2$ and $Q^2 = 2.5\ \mathrm{GeV}^2$.

results for CFFs

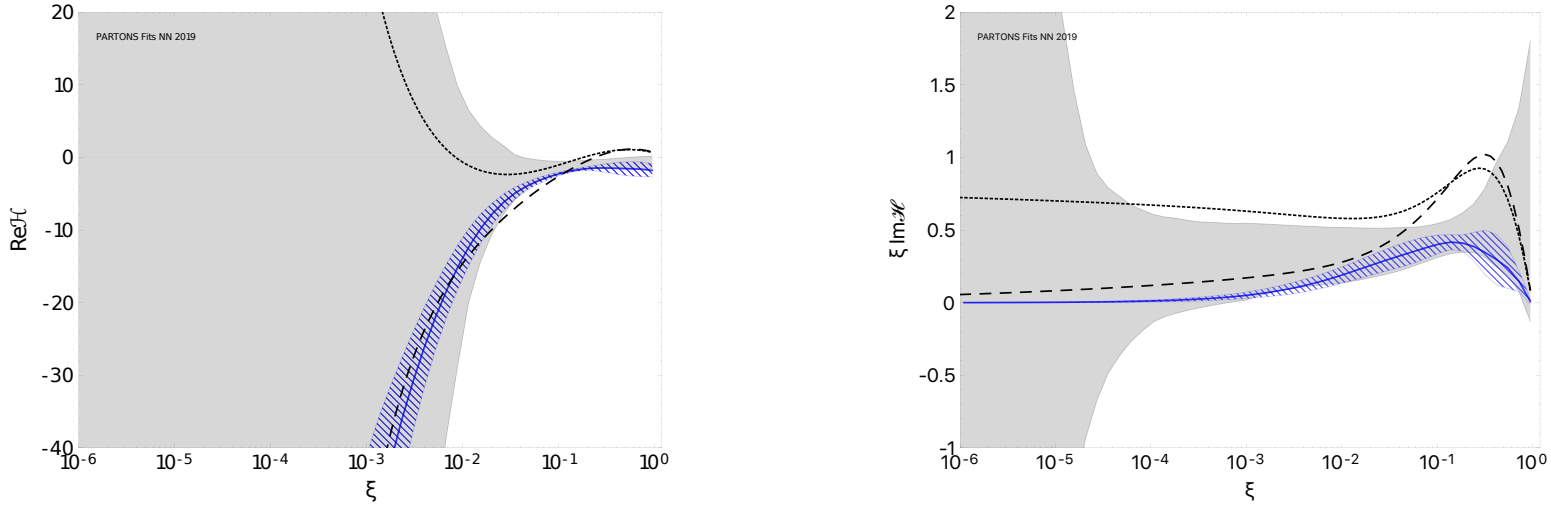

Figure: Real (left) and imaginary (right) parts of the CFF $\mathcal{H}$ as a function of ξ for $t = -0.3\ \mathrm{GeV}^2$ and $Q^2 = 2\ \mathrm{GeV}^2$. The blue solid line surrounded by the blue hatched band denotes the result of our previous analysis.

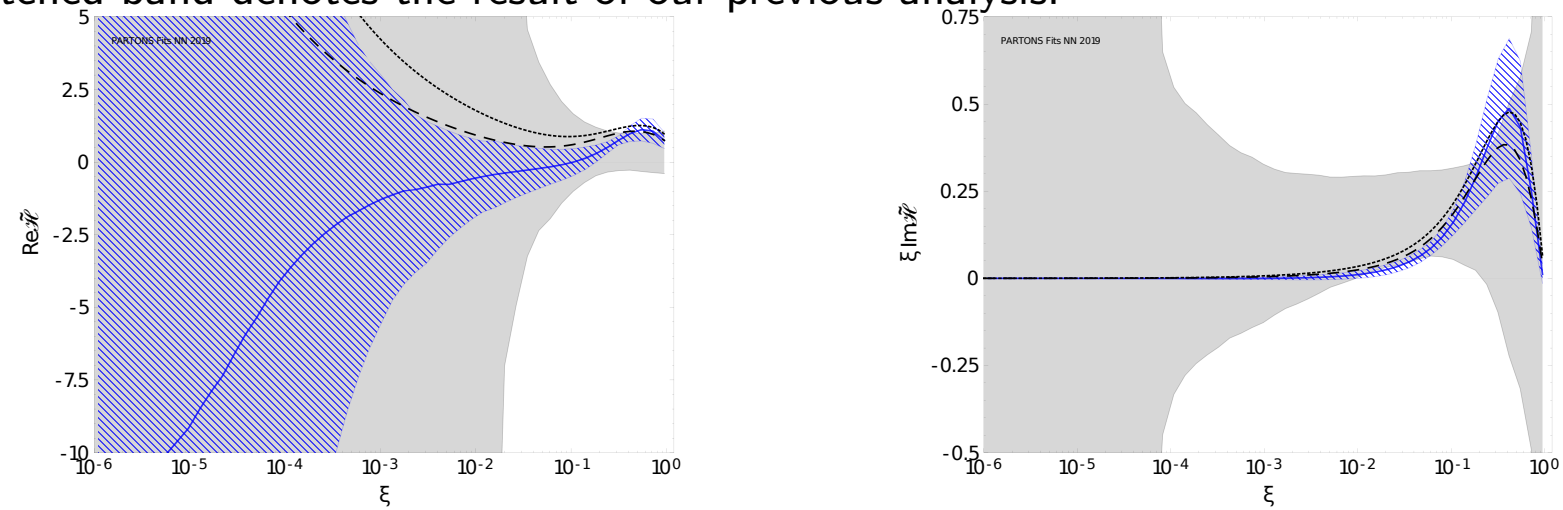

Figure: Real (left) and imaginary (right) parts of the CFF $\widetilde{\mathcal{H}}$ as a function of ξ for $t = -0.3\ \mathrm{GeV}^2$ and $Q^2 = 2\ \mathrm{GeV}^2$.

Subtraction Constant

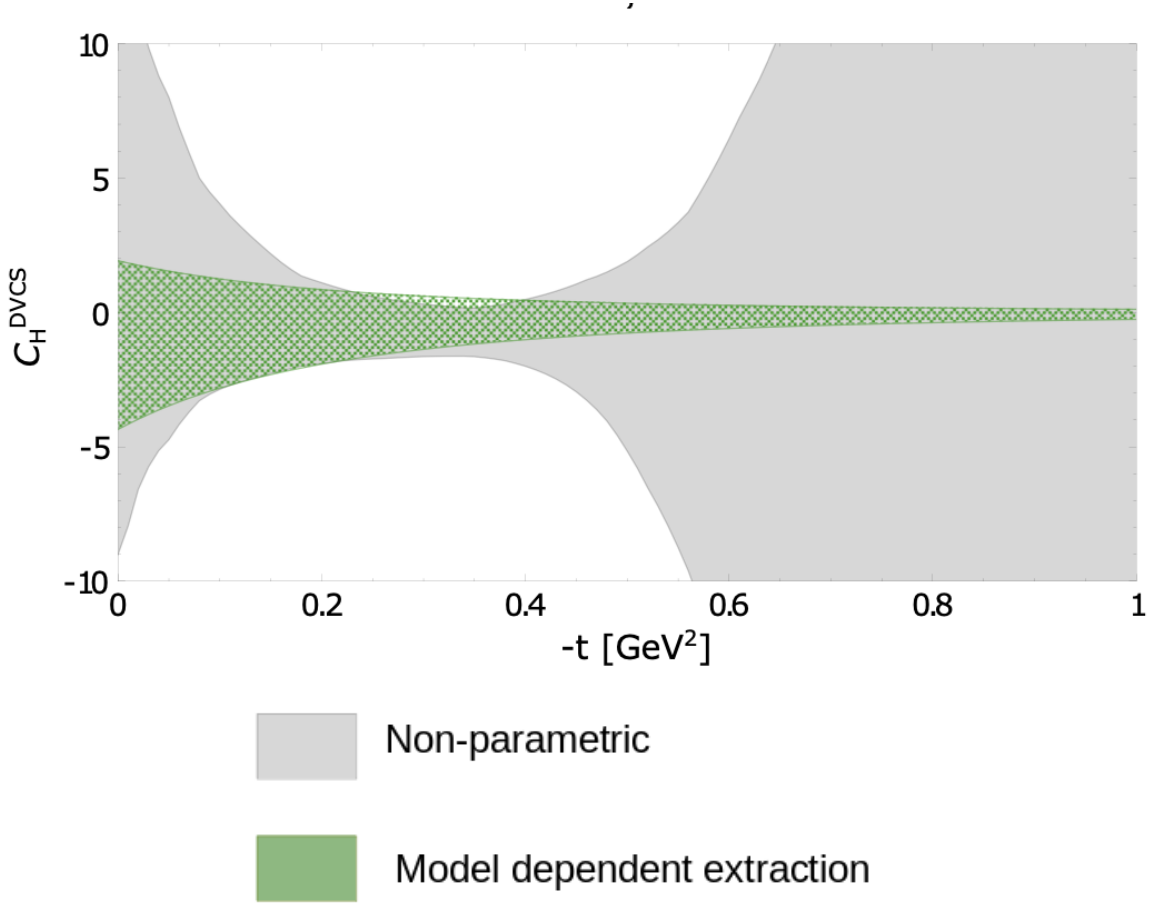

Status of DVCS fits

- Other groups:
  - Kumericki, Muller,
  - Guidal, Vanderhaeghen, Dupre,
  - Burkert, Elouadrhiri, Girod
  - Liuti, Kriesten et al.
- Most fits still at LO and LT - effectively Compton Form Factors fits
- More channels needed:
  - DVCS on neutron
  - Timelike Compton Scattering (TCS)
  - Double Deeply Virtual Compton Scattering (DDVCS)
  - Deeply Virtual Meson Production
  - Photoproduction of heavy mesons
- We need to go from $x = \xi$ line - DDVCS
- higher twist needed, especially for JLab kinematics
- Switch from CFFs to GPDs - flexible modelling,
- NLO fits! (first attempts for low-x by Kumericki, Mueller, Lautenschlager)

we can also study timelike DVCS

Berger, Diehl, Pire, 2002

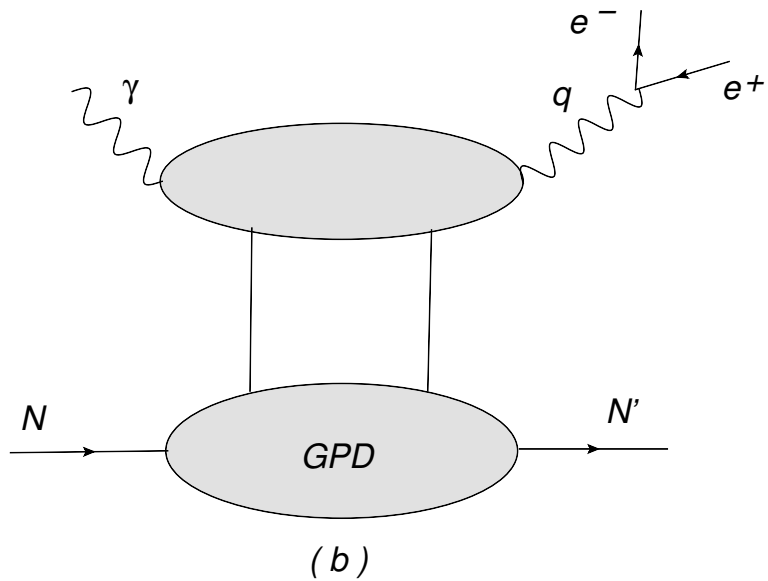

Figure: Timelike Compton Scattering (TCS): $\gamma N \to l^+ l^- N'$

Why TCS:

- universality of the GPDs
- another source for GPDs (special sensitivity on real part of GPD H),
- spacelike-timelike crossing (different analytic structure - cut in Q^2)

Spacelike vs Timelike

D.Mueller, B.Pire, L.Szymanowski, J.Wagner, Phys.Rev.D86, 2012.

Thanks to simple spacelike-to-timelike relations, we can express the timelike CFFs by the spacelike ones in the following way:

$$
\begin{aligned}
{}^{T}\mathcal{H} &\overset{\text{LO}}{=} {}^{S}\mathcal{H}^{*}\,, \\
{}^{T}\widetilde{\mathcal{H}} &\overset{\text{LO}}{=} -{}^{S}\widetilde{\mathcal{H}}^{*}\,, \\
{}^{T}\mathcal{H} &\overset{\text{NLO}}{=} {}^{S}\mathcal{H}^{*} - i\pi\,\mathcal{Q}^{2}\frac{\partial}{\partial\mathcal{Q}^{2}}{}^{S}\mathcal{H}^{*}\,, \\
{}^{T}\widetilde{\mathcal{H}} &\overset{\text{NLO}}{=} -{}^{S}\widetilde{\mathcal{H}}^{*} + i\pi\,\mathcal{Q}^{2}\frac{\partial}{\partial\mathcal{Q}^{2}}{}^{S}\widetilde{\mathcal{H}}^{*}\,.
\end{aligned}
$$

The corresponding relations exist for (anti-)symmetric CFFs $\mathcal{E}$ ($\widetilde{\mathcal{E}}$).

DVCS vs TCS CFFs

O. Grocholski, H. Moutarde, B. Pire, P. Sznajder, J. Wagner, Eur.Phys.J. C80 (2020)

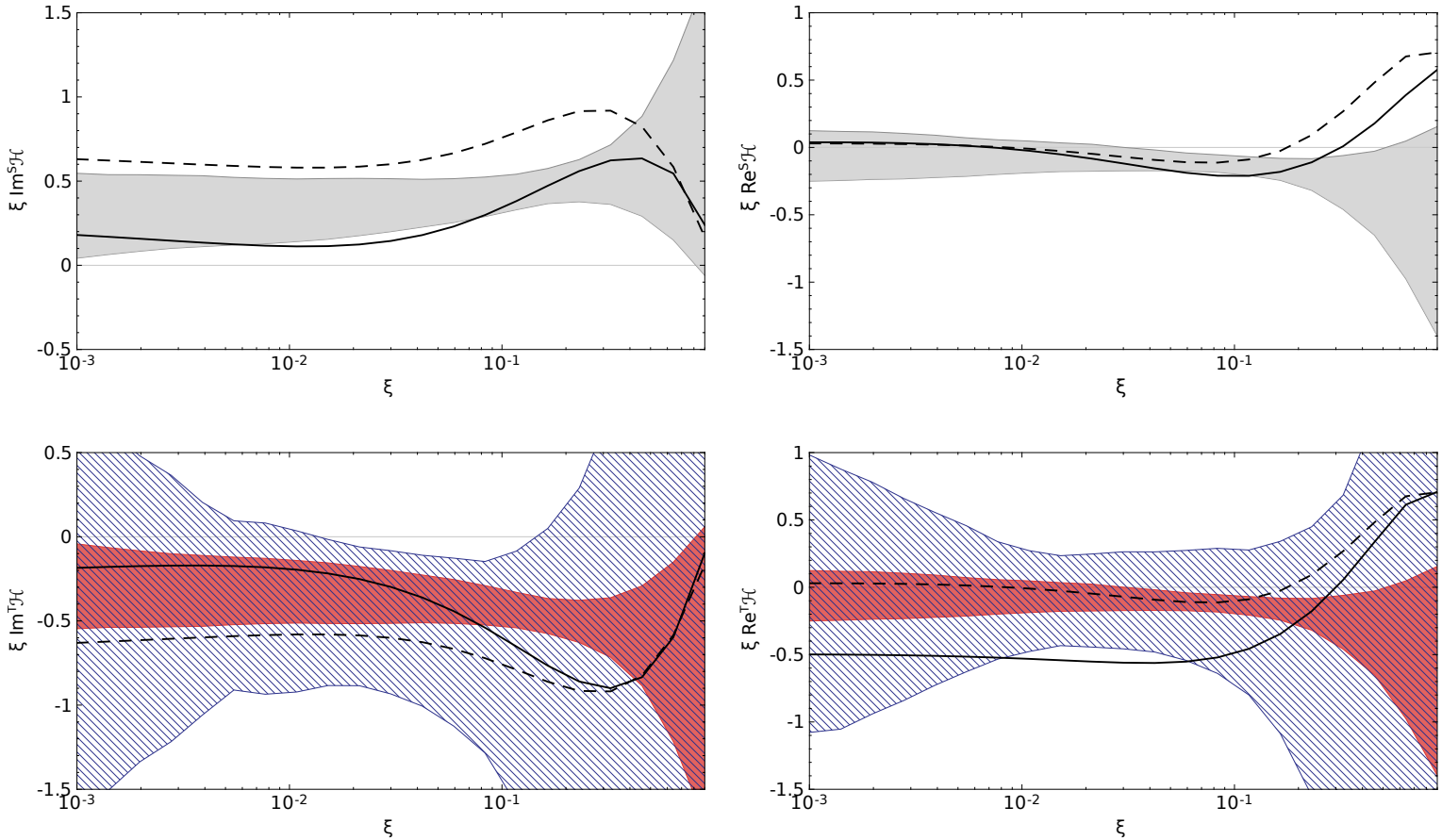

Figure: Imaginary (left) and real (right) part of DVCS (up) and TCS (down) CFF for $Q^2 = 2$ GeV^2 and $t = -0.3$ GeV^2 as a function of ξ. The shaded red (dashed blue) bands correspond to the data-driven predictions coming from the ANN global fit of DVCS data and they are evaluated using LO (NLO) spacelike-to-timelike relations. The dashed (solid) lines correspond to the GK GPD model evaluated with LO (NLO) coefficient functions.

Circular asymmetry

The photon beam circular polarization asymmetry:

$$A_{CU} = \frac{\sigma^+ - \sigma^-}{\sigma^+ + \sigma^-} \sim Im(H)$$

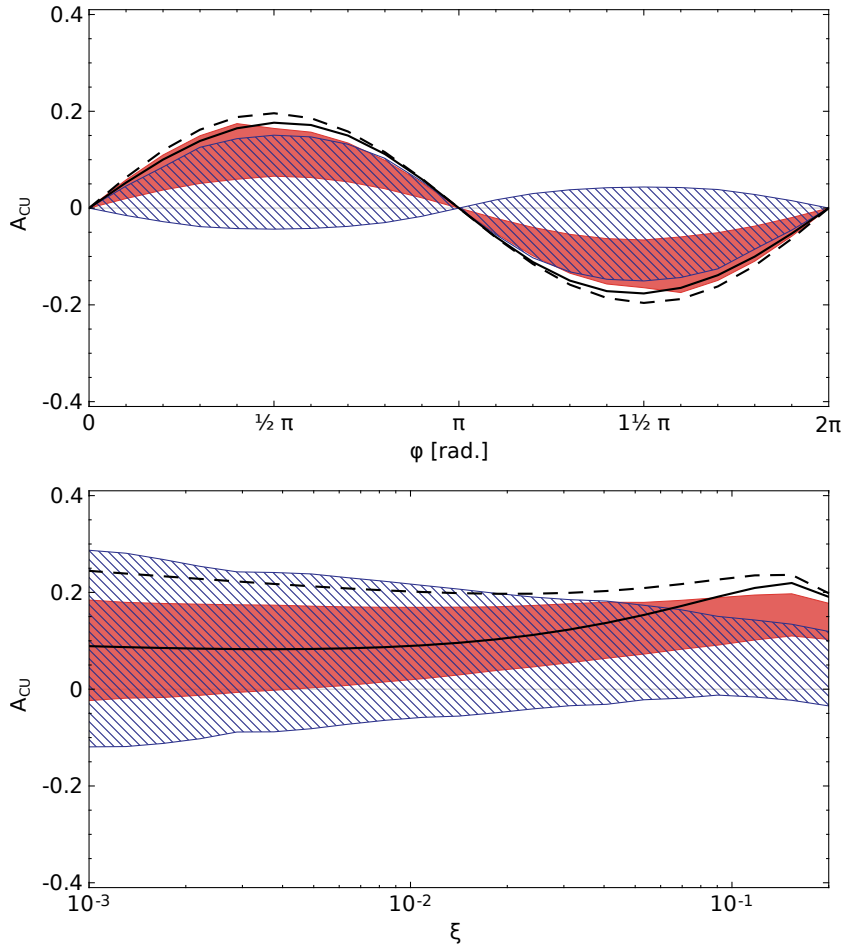

Figure: Circular asymmetry A_{CU} evaluated with LO and NLO spacelike-to-timelike relations for $Q'^2 = 4$ GeV^2, $t = -0.1$ GeV^2 and (left) $E_\gamma = 10$ GeV as a function of ϕ (right) and $\phi = \pi/2$ as a function of ξ. The cross sections used to evaluate the

Experimental status

- First measurement: P. Chatagnon et al. (CLAS), PRL 127, 262501 (2021)

PHYSICAL REVIEW LETTERS **127,** 262501 (2021)

First Measurement of Timelike Compton Scattering

P. Chatagnon,[20,*] S. Niccolai,[20] S. Stepanyan,[36] M. J. Amaryan,[29] G. Angelini,[12] W. R. Armstrong,[1] H. Atac,[35] C. Ayerbe Gayoso,[44,†] N. A. Baltzell,[36] L. Barion,[13] M. Bashkanov,[42] M. Battaglieri,[36,15] I. Bedlinskiy,[25] F. Benmokhtar,[7] A. Bianconi,[39,19] L. Biondo,[15,18,40] A. S. Biselli,[8] M. Bondi,[15] F. Bossù,[3] S. Boiarinov,[36] W. J. Briscoe,[12] W. K. Brooks,[37,36]

- TCS has the same final state as J/ψ, already measured in UPCs! LHCb, CMS, ALICE, AFTER

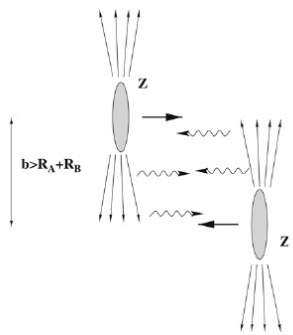

$$\sigma^{AB} = \int dk_A \frac{dn^A}{dk_A} \sigma^{\gamma B}(W_A(k_A)) + \int dk_B \frac{dn^B}{dk_B} \sigma^{\gamma A}(W_B(k_B))$$

Double DVCS

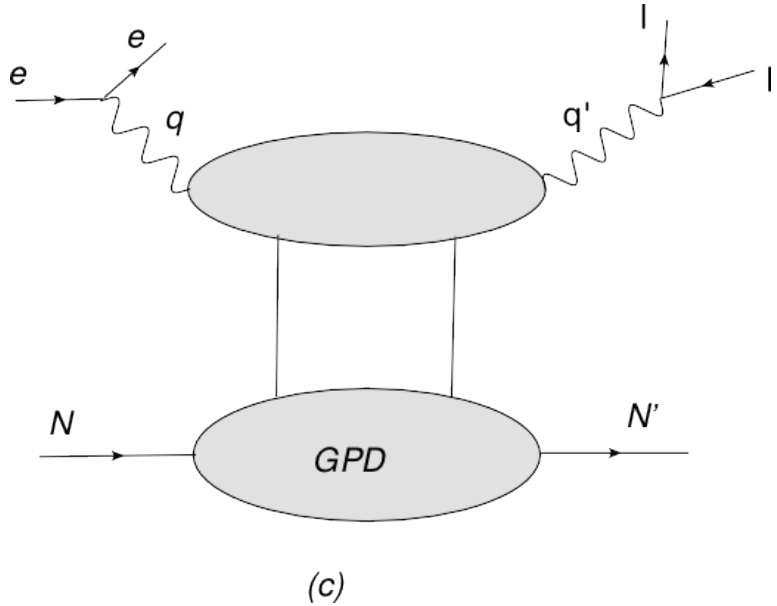

Figure: Double Deeply Virtual Compton Scattering (DDVCS): $\gamma N \to l^+ l^- N'$

$$\gamma^*(q_{in})N(p) \to \gamma^*(q_{out})N'(p')$$

Variables, describing the processes of interest in this generalized Bjorken limit, are the scaling variable ξ and skewness $\eta > 0$:

$$\xi = -\frac{q_{out}^2 + q_{in}^2}{q_{out}^2 - q_{in}^2}\eta\,, \quad \eta = \frac{q_{out}^2 - q_{in}^2}{(p+p')\cdot(q_{in}+q_{out})}\,.$$

- DDVCS: $q_{in}^2 < 0\,, \quad q_{out}^2 > 0\,, \quad \eta \neq \xi$
- DVCS: $q_{in}^2 < 0\,, \quad q_{out}^2 = 0\,, \quad \eta = \xi > 0$
- TCS: $q_{in}^2 = 0\,, \quad q_{out}^2 > 0\,, \quad \eta = -\xi > 0$

Coefficient functions and Compton Form Factors

CFFs are the GPD dependent quantities which enter the amplitudes. They are defined through relations:

$$\mathcal{A}^{\mu\nu}(\xi,\eta,t) = -e^2 \frac{1}{(P+P')^+}\,\bar{u}(P')\Bigg[g_T^{\mu\nu}\left(\mathcal{H}(\xi,\eta,t)\,\gamma^+ + \mathcal{E}(\xi,\eta,t)\,\frac{i\sigma^{+\rho}\Delta_\rho}{2M}\right) + i\epsilon_T^{\mu\nu}\left(\widetilde{\mathcal{H}}(\xi,\eta,t)\,\gamma^+\gamma_5 + \widetilde{\mathcal{E}}(\xi,\eta,t)\,\frac{\Delta^+\gamma_5}{2M}\right)\Bigg] u(P)\,,$$

,where:

$$\begin{aligned}
\mathcal{H}(\xi,\eta,t) &= +\int_{-1}^{1} dx \left(\sum_q T^q(x,\xi,\eta)H^q(x,\eta,t) + T^g(x,\xi,\eta)H^g(x,\eta,t)\right)\\
\widetilde{\mathcal{H}}(\xi,\eta,t) &= -\int_{-1}^{1} dx \left(\sum_q \widetilde{T}^q(x,\xi,\eta)\widetilde{H}^q(x,\eta,t) + \widetilde{T}^g(x,\xi,\eta)\widetilde{H}^g(x,\eta,t)\right).
\end{aligned}$$

LO

- DVCS vs TCS

$$
\begin{aligned}
{}^{DVCS}T^q &= -e_q^2 \tfrac{1}{x+\eta-i\varepsilon} - (x \to -x) = \quad ({}^{TCS}T^q)^* \\
{}^{DVCS}\tilde{T}^q &= -e_q^2 \tfrac{1}{x+\eta-i\varepsilon} + (x \to -x) = \quad -({}^{TCS}\tilde{T}^q)^*
\end{aligned}
$$

$$
{}^{DVCS}Re(\mathcal{H}) \sim P \int \frac{1}{x \pm \eta} H^q(x,\eta,t)\,, \qquad {}^{DVCS}Im(\mathcal{H}) \sim i\pi H^q(\pm\eta,\eta,t)
$$

- DDVCS

$$
{}^{DDVCS}T^q = -e_q^2 \frac{1}{x+\xi-i\varepsilon} - (x \to -x)
$$

$$
{}^{DDVCS}Re(\mathcal{H}) \sim P \int \frac{1}{x \pm \xi} H^q(x,\eta,t)\,, \qquad {}^{DVCS}Im(\mathcal{H}) \sim i\pi H^q(\pm\xi,\eta,t)
$$

DDVCS can provide unique information, but is very challenging experimentally. But recent measurement of TCS should also make us more optimistic about DDVCS!

We need muon detection!

Other processes

- Hard photo- and electroproduction of a diphoton with a large invariant

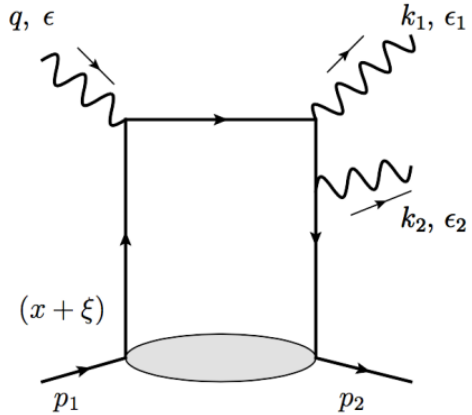

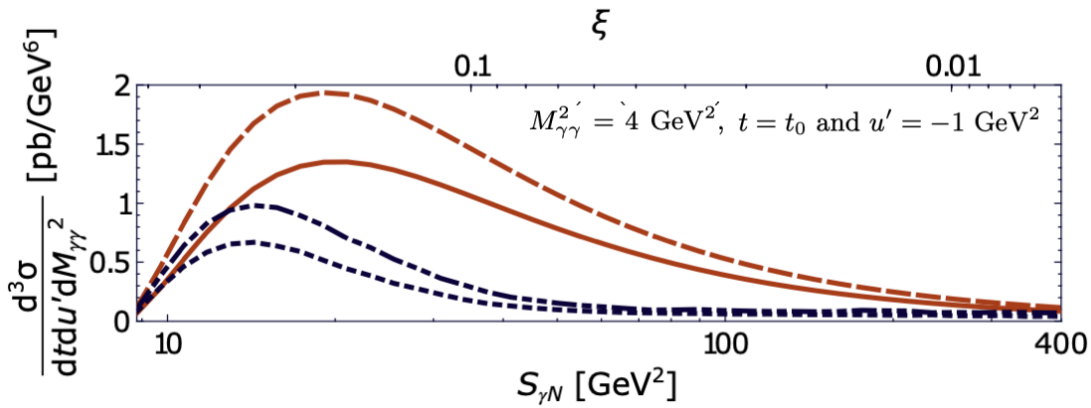

- Meson production - important, but not for today :)

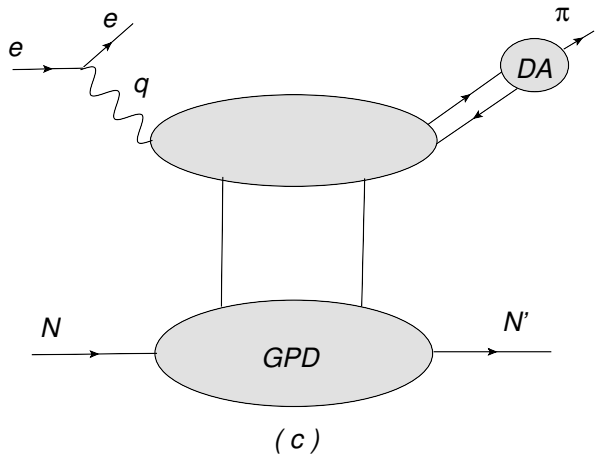

(c)

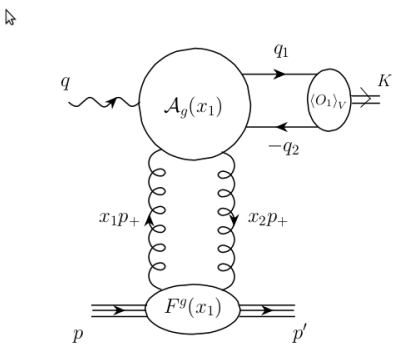

Figure 1: Kinematics of heavy vector meson photoproduction.

Summary

- Fairly accurate descriptions of DVCS data exist:
  - with parametrizations and neural networks,
  - mostly on the LO+LT level, effectively Compton Form Factors fits
  - extraction of GPDs from DVCS CFFs is **model dependent**
- Multi-channel analysis needed:
  - Deeply Virtual Meson Production
  - First data on Timelike Compton Scattering
  - DVCS/TCS on neutrons planned/measured at JLAB
  - Heavy Vector Mesons, specially sensitive to gluon GPDs.
- We **have to** get info about GPDs at $x \neq \xi$:
  - Double DVCS - difficult experimentally, but provide unique information
  - Lattice
- Need for open source tools